Epm2a suppresses tumor growth in an immunocompromised host by inhibiting Wnt signaling

Yin Wang,[1,3,5] Yan Liu,[1,3,5] Cindy Wu,[1] Huiming Zhang,[1,5] Xincheng Zheng,[1,5] Zhi Zheng,[4] Terrence L. Geiger,[2] Gerard J. Nuovo,[1] Yang Liu,[1,5,*] and Pan Zheng[1,5,*]

[1] Division of Cancer Immunology, Department of Pathology, and Comprehensive Cancer Center, Ohio State University Medical Center, Columbus, Ohio 43210
[2] Department of Pathology, St. Jude Children's Research Hospital, Memphis, Tennessee 38105
[3] These authors contributed equally to this work.
[4] Present address: 289 Merrill Avenue, Fremont, California 94539.
[5] Present address: Division of Immunotherapy, Department of Surgery and Pathology, and Comprehensive Cancer Center, University of Michigan, Michigan 48109.
*Correspondence: panz@umich.edu (P.Z.); yangl@umich.edu (Y.L.)

Summary

The genetic mechanisms responsible for increased incidence of lymphoma in immunocompromised individuals have not been fully elucidated. We show that, in a line of TCR transgenic TG-B mice, an insertional mutation in one allele of the *Epm2a* locus and epigenetic silencing of another led to a high rate of lymphoma with early onset. Overexpressing *Epm2a* suppressed the growth of established tumor cells and the development of lymphoma in the TG-B mice, while specific silencing of the locus increased tumorigenesis in the immune-deficient host. Downregulation of *Epm2a* expression is widespread among mouse and human lymphoma cell lines. *Epm2a*-encoded laforin is a phosphatase for GSK-3β and an important repressor in the Wnt signaling pathway. Inactivation of *Epm2a* resulted in increased Wnt signaling and tumorigenesis.

Introduction

Significant increases in cancer rate have been reported in immune-deficient individuals, including those infected with the human immune-deficient virus (HIV) (Boshoff and Weiss, 2002) and transplantation patients under constant immune suppression (Penn, 1995, 1996). These observations support the notion that T cell-mediated immunity serves as a major barrier for the development of cancer (Dunn et al., 2002). On the other hand, mice with defective T cell immunity, such as nude mice (Rygaard and Povlsen, 1974), do not appear to have a major increase in the rate of spontaneous cancer. An intriguing possibility is that other genetic defects may act in concert with immunodeficiency to cause cancer. While defects in bona fide cancer suppressor genes have been shown to synergize with immune deficiency in the development of spontaneous cancer (Liao and Van Dyke, 1999; Liao et al., 1998), it is unknown whether a different class of cancer suppressor genes exists that can cause cancer primarily in an immune-deficient host.

The T cell receptor (TCR) transgenic mice have random cointegration of the genes encoding for the α and β chains of the TCR into the genome. Because of the allelic exclusion, expression of the transgenic TCR represses the endogenous TCR. As a result, the host is substantially devoid of T cells with the capacity to combat cancer cells. Nevertheless, the development of cancer in TCR transgenic mice has rarely been observed. Occasionally, thymoma was reported in TCR transgenic mice late in life (around 2 years of age) (Reimann et al., 1994). This general experience is consistent with the notion that limiting TCR repertoire is insufficient to cause cancer development. We made a serendipitous observation that one line of TCR transgenic mice, called TG-B mice (Geiger et al., 1992), developed T cell lymphoma with almost 100% penetrance and a median survival of 6 months. Since lymphoma of such severity is unprecedented in TCR transgenic mice, we carried out position cloning in order to identify the genetic basis for the malignancy. We found that the transgenes were inserted in intron 1 of *Epm2a*, which was initially identified as one of the causative genes for progressive myoclonus epilepsy (Ganesh et al., 1999, 2000; Minassian et al., 1998). The function of *Epm2a* as a tumor suppressor is further confirmed by specific silencing and by transfection studies. Moreover, we have found that laforin is a phosphatase for GSK-3β and *Epm2a* inactivation is associated with enhanced Wnt signaling. The activated Wnt signaling pathway is essential for the development of cancer in an immunodeficient host. Our results demonstrate that *Epm2a* is a tumor suppressor gene in an

SIGNIFICANCE

Immune surveillance is an important concept in cancer biology and immunology. An important issue is whether specific genetic alteration may be associated with cancer development in an immunocompromised host. Our data showed that *Epm2a* alteration may be such a genetic factor and thus provide strong support for the concept of immune surveillance. Moreover, identification of laforin as a regulator for Wnt signaling and GSK-3β phosphorylation may suggest a broad function of laforin in cellular physiology.

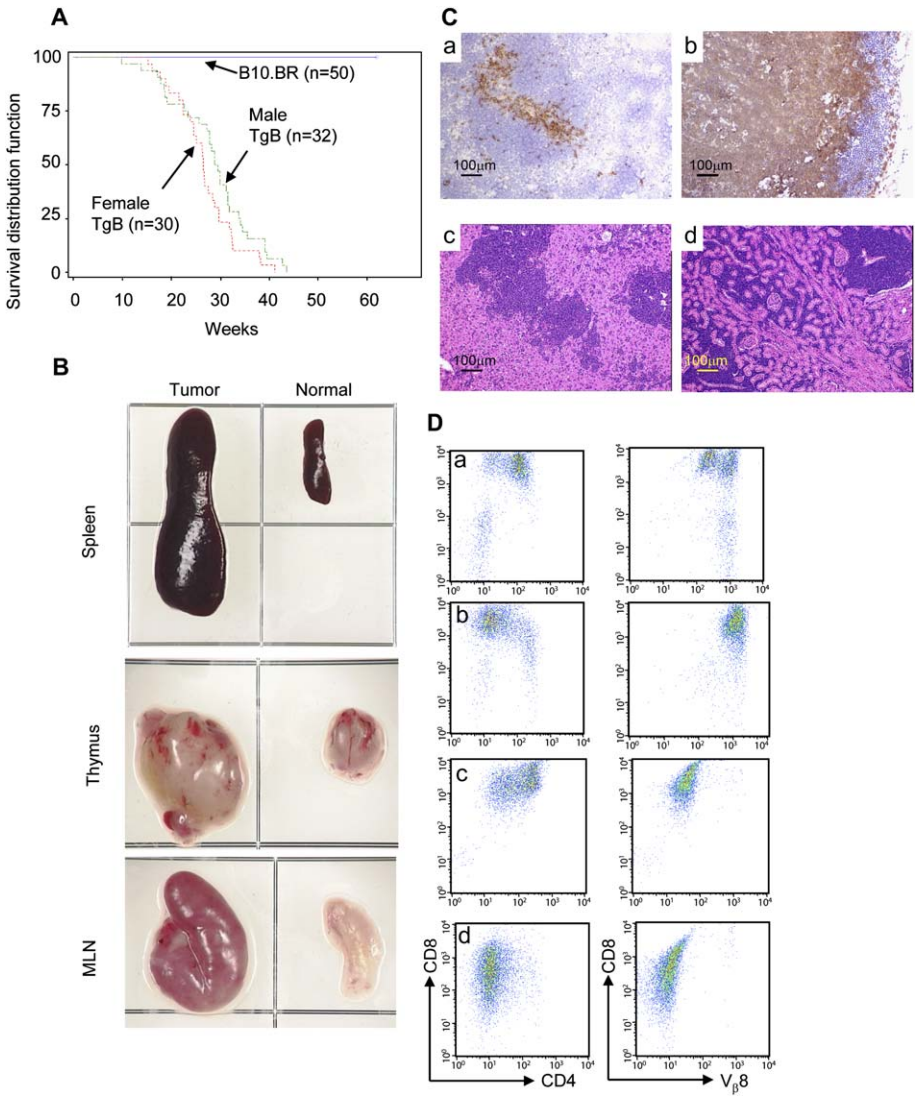

Figure 1. A transgenic mouse line developed lymphoma with high penetrance and early lethality

A: The survival distribution function among B10.BR and TG-B male and female mice. The incidence of lymphoma is significantly higher among TG-B in comparison to wild-type ($p < 0.0001$) mice.

B: Enlargement of spleen, thymus, and mesenteric lymph node (MLN) in a TG-B mouse with tumor (left panels). Organs from a TG-B mouse that have not developed tumor are shown as controls.

C: Immunohistochemical staining of anti-Thy1 in non-Tg spleen showing normal T cell distribution (**Ca**) and in spleen from TG-B mouse with lymphoma showing that the entire spleen was infiltrated by large lymphoblastic T cells (**Cb**). H&E sections of liver (**Cc**) and kidney (**Cd**) of the tumor-bearing TG-B mice show the infiltration of lymphoma cells in organs.

D: Immunophenotypes of the lymphomas by flow cytometry. Normal thymic cells or lymphomatous thymic cells were stained with antibodies against CD4, CD8, and Vβ8. **Da:** Normal thymic cells showed the TCR transgenic phenotype with skewed $CD8^+$ single-positive cells and predominantly $V\beta8^+$ transgenic cells (Geiger et al., 1992); **Db:** a thymoma with predominantly high $V\beta8^+$ mature single $CD8^+$ cells; **Dc:** a thymoma with immature $CD4^+CD8^+$ cells and lower levels of Vβ8; **Dd:** a lymphoma with immature single positive (ISP) $CD8^+$ (a T cell development stage between double-negative and double-positive) without any Vβ8 expression.

immunocompromised host and an important modulator of Wnt signaling.

Results

Transgene insertion to and hypermethylation of the *Epm2a* gene induces spontaneous lymphoma in TG-B transgenic mice

The TG-B transgenic mice used in this study have rearranged T cell receptor α and β chain genes isolated from a clonal $CD8^+$ cytotoxic T cell line. The TCR transgenes were integrated into the genome of the B10.BR ($H\text{-}2^k$) mice (Geiger et al., 1992). Surprisingly, the heterozygous TG-B mice had a high incidence of lymphoma regardless of sex. The maximal survival time for TG-B mice was 9 months, with a median survival time of 6 months (Figure 1A). The lymphoma was first seen in lymphoid organs, including the thymus, spleen, and lymph nodes (Figure 1B). As the cancer progressed, the tumor cells infiltrated other organs, such as the liver, kidney (Figure 1C), lung, pancreas, intestines, and salivary glands (data not shown). The immunophenotype of the T cell lymphoma varied between animals, suggesting that transformation occurred at various stages in T cell development (Figure 1D).

We determined the integration site of the transgene by fluorescence in situ hybridization (FISH) using a biotin-labeled DNA fragment probe from the TCRα chain constant region (Heng et al., 1992). A strong signal was identified on one copy of chromosome 10 (Figure 2A). The strong signal was localized to region 10A2 based on the summary of ten images (data not shown). Two weaker FISH signals were detected, one on each copy of chromosome 14, which was consistent with the location of the endogenous TCRα genes. Fine mapping of integration sites was performed by the TOPO Walker method (Shuman, 1994). PCR products using the TOPO Linker primers and the gene-specific sequence primers from both the 3′ and 5′ termini of the TCRα and TCRβ transgenes were cloned and sequenced. Three independent experiments revealed that the TCRα transgene was inserted into the intron 1 of *Epm2a*, which encodes laforin, a dual specificity protein phosphatase (Figure 2B) (Minassian et al., 1998; Serratosa et al., 1999). Further PCR analysis using primers corresponding to the 3′ terminus of the TCRα transgene and the 5′ terminus of the TCRβ transgene confirmed that these genes were cointegrated into chromosome 10 in

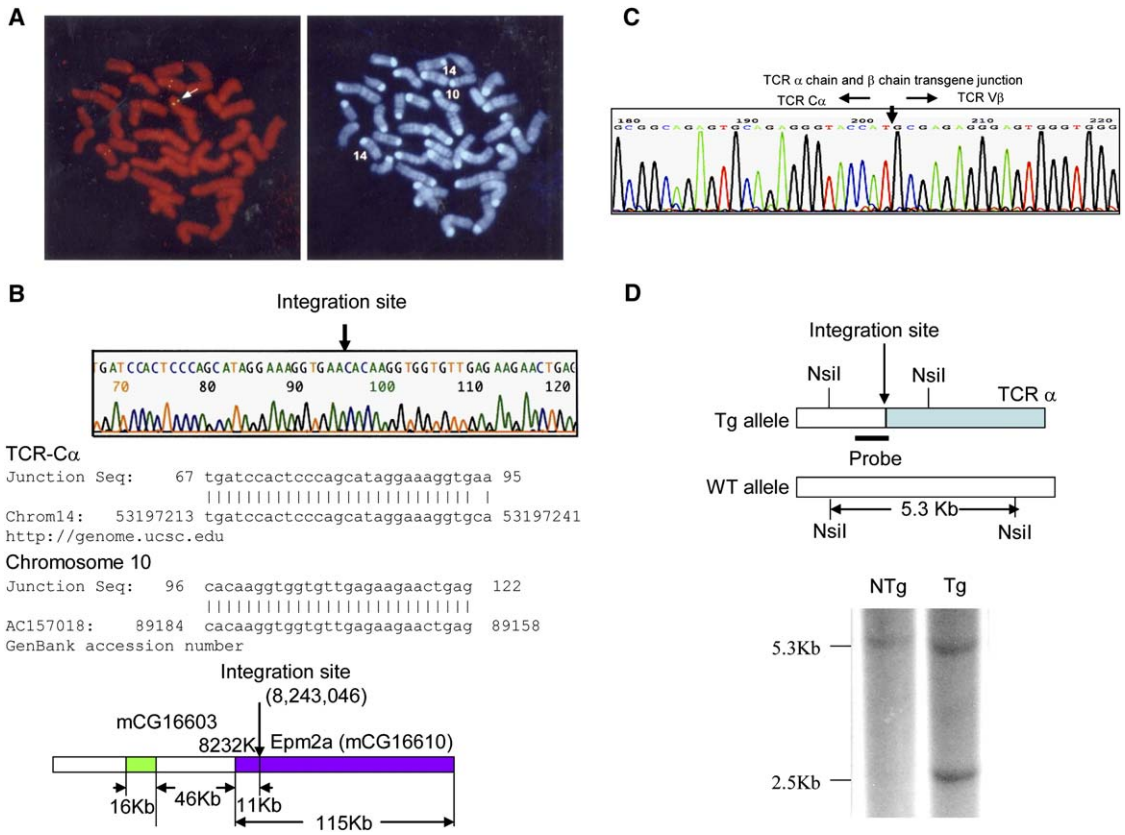

Figure 2. Identification of the integration site of the TCR transgene

A: Cytogenetic analysis of TCR gene localization by FISH. The probe used was the constant region of the TCRα chain. The location of the transgene is indicated by an arrow in the FISH image (left panel), and the positions of chromosomes 10 and 14 are marked in the DAPI staining (right panel). The signals in chromosome 14 reflect the location of the endogenous TCRα loci. The signal in chromosome 10 is the transgene insertion locus.

B: Fine mapping of the TCR integration site. A representative chromatogram depicting the junction region sequence is shown at the top, and the alignments of this sequence to those of mouse chromosomes 10 and 14 are shown in the middle. The bottom panel shows a portion of mouse chromosome 10A2 surrounding the integrating site as annotated in the Celera database; note that the integrating site is in intron 1 of *Epm2a*.

C: Chromatogram depicting the junctional sequence of TCRα and β constructs.

D: Confirmation of the integration site by Southern blot. The restriction enzyme map of endogenous and Tg alleles and a Southern blot autograph are shown.

TG-B mice (Figure 2C). The integration was confirmed by Southern blot using the sequence adjacent to the integration site as probe (Figure 2D). Additional chromosomal walking with the β chain probe failed to identify other integration sites for the TCRβ construct (data not shown).

We examined the expression of the *Epm2a* gene in the thymi of nontransgenic mice (NTg), transgenic littermates with no tumor (Tg), and transgenic mice that developed lymphoma (Tg-Tu). Based on RT-PCR amplification of full-length transcript, *Epm2a* was expressed at significant levels in nontransgenic and transgenic littermates. However, its expression in Tg-Tu lymphoma cells was greatly reduced (Figure 3A). RNase protection assay using an *Epm2a* probe spanning exons 3 and 4 did not find any *Epm2a* transcript containing either one of the two exons in Tg-Tu lymphoma (Figure 3B). Using a polyclonal antibody against laforin, we showed that laforin was expressed in Tg mice with approximately half of the amount in NTg mice but was absent in the transgenic mice that developed lymphoma (Tg-Tu) (Figure 3C). Moreover, we observed downregulation of laforin in the majority of the murine T and B cell lymphoma cell lines that we tested (Figure 3D). Thus, tumorigenesis was consistently associated with altered laforin gene expression. Interestingly, the high tumor incidence and lack of laforin that are documented in Figure 1A were observed in heterozygous mice. To determine whether loss of heterozygocity is responsible for tumor development, we genotyped tumor cells for the presence of wild-type and disrupted *Epm2a* alleles. As shown in Figure 3E, all tumor cells had both wild-type and disrupted alleles (Figure 3E).

The *Epm2a* gene contains a 1.2 kb 5′-CpG island that spans the promoter region, exon 1, and part of intron 1 (Figure 4A). To determine if DNA hypermethylation was an epigenetic mechanism for laforin gene downregulation in TG-B lymphoma, we treated the genomic DNA with bisulfite and sequenced four PCR products covering 102 CpG dinucleotides within the 5′-CpG island. Based on methylation-mediated protection of C>T conversion by the sodium bisulfite, we identified the methylated CpG dinucleotides. As illustrated in Figure 4B, extensive hypermethylation was found in the *Epm2a* gene of all six lymphoma samples. In contrast, none of the normal thymi had methylation in this region.

Our survey of multiple lymphoma cell lines revealed that downregulation of *Epm2a* gene expression was widespread among murine lymphomas (Figures 3E and 4C). We compared three nonlymphoid tumor cell lines with three T lymphoma cell lines for 5-aza-2′-deoxycytidine (5-Aza-dC)-induced *Epm2a*

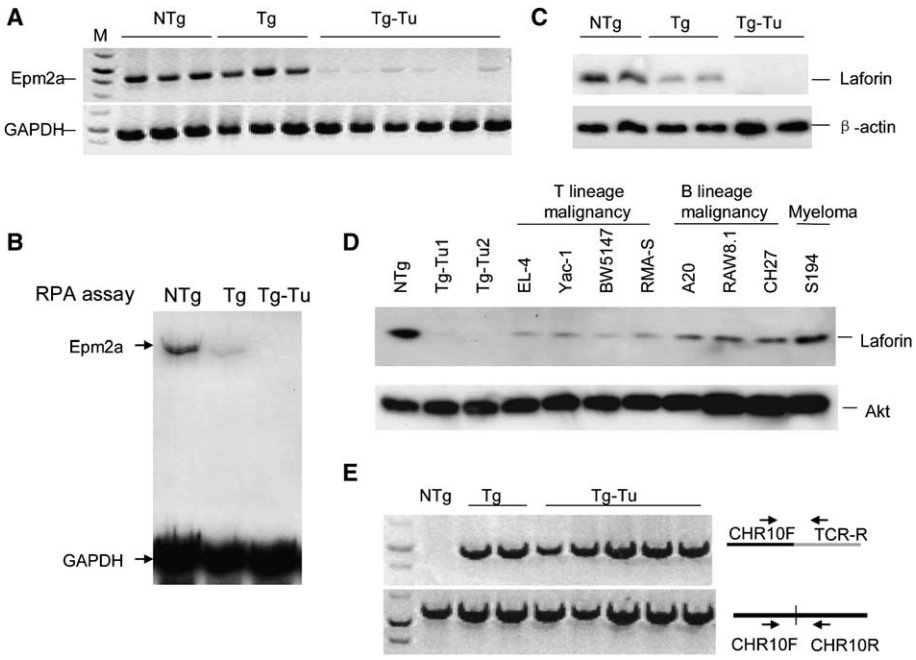

Figure 3. Reduced expression of laforin in lymphoma

A: Defective expression of *Epm2a* mRNA in transgenic mice with lymphoma (Tg-Tu), but not in the nontransgenic littermates (NTg), or in young transgenic mice that have not yet developed lymphoma (Tg).

B: RNase protection assay showing no truncated Epm2a transcript in Tg-Tu. The probe used spanned exons 3 and 4.

C: Absence of laforin protein expression in Tg-Tu lymphoma cells and reduction of laforin expression in thymi from young transgenic (Tg) mouse by Western blot.

D: Downregulation of laforin protein in multiple murine malignancies of T and B cell lineages. The thymocytes from a nontransgenic littermate (Ntg) and two transgenic mice with lymphoma (Tg-Tu) were examined as control. The malignant cell lines used were EL4, YAC-1, BW5147, RMA-S (T cell lymphoma), A20, RAW8.1, CH27 (B cell lymphoma), and S194 (myeloma). Data shown are representative of three independent experiments.

E: Thymoma in TG-B mice retained both wild-type and disrupted *Epm2a* alleles. Genomic DNA was isolated from NTg, Tg, and Tg-Tu thymi. PCR reactions were performed using a forward primer in chromosome 10, paired with a reverse primer from chromosome 10 or a reverse primer from TCRα chain constant region.

expression. As shown in Figure 4C, treatment with methyl-transferase inhibitor 5-Aza-dC increased *Epm2a* expression in three T lymphoma cell lines but had little effect on three nonlymphoid tumor cell lines that had relatively high levels of *Epm2a* expression. To test whether hypermethylation of the *Epm2a* promoter was responsible for repression of the *Epm2a* gene, we determined the *Epm2a* promoter hypermethylation by quantitative real-time PCR based on susceptibility to a methylation-sensitive restriction enzyme, SacII. *Epm2a* promoter region DNA from mouse no. 4012 had been treated with bisulfite and sequenced to show there was 100% CpG methylation, but promoter region from mouse no. 11992 was not methylated (Figure 4B). Genomic DNA from mouse 4012 and mouse 11992 was used as positive and negative controls in this assay. As shown in Figure 4D, real-time PCR showed similar amplification between three T cell lymphomas and control mouse 4012, indicating that T cell lymphomas had similar hypermethylation in the *Epm2a* promoter region and their genomic DNA was resistant to SacII digestion. In contrast, genomic DNA from three nonlymphoid tumor cell lines was not methylated and was sensitive to SacII digestion; therefore, real-time PCR failed to amplify the SacII fragmented *Epm2a* promoter region. These data are consistent with the notion that hypermethylation is responsible for *Epm2a* downregulation among T lymphomas.

Inactivation of the *Epm2a* locus is necessary and sufficient to initiate cancer development

There are two genes within 300 kb of the transgene integration site. The proximal gene is 56 kb away from the integration site and encodes a protein that contains an F box domain (mCG16603), while the other gene is 135 kb from the integration site (mCG140768) (Figure 5A). We performed RNase protection assay to determine the mRNA expression of these two genes. The expression level of the distal gene (mCG140768) was not affected by the transgene or lymphoma development, while the expression of the proximal gene (mCG16603) was upregulated by the transgene regardless of lymphoma formation (Figure 5B). We tested this possibility by producing eight independent founders of transgenic mice that expressed mCG16603 under the control of a proximal *lck* promoter, which resulted in high levels of expression in the thymus. None of the mice developed lymphoma in up to 22 months of observation (Figure 5C). The offspring of one of the founders were observed over a 1 year period. Although mCG16603 was expressed at much higher levels than in the TG-B mice (Figure 5D), no lymphoma was observed in the 12 mice observed over a 45–61 week period (Figure 5C). Thus, lymphoma development in the TG-B mice was unlikely caused by the abnormal expression of other genes near the integration site, although the possibility that the overexpression of mCG16603 may promote cancer development in this model cannot be completely ruled out at this stage.

To test whether inactivation of the *Epm2a* gene is sufficient to cause abnormal cell growth, we tested the consequences of silencing the *Epm2a* gene in the bone marrow stem cells in both methylcellulose assay in vitro and bone marrow reconstitution in vivo. Unmanipulated murine bone marrow had a finite ability to self-renew in methylcellulose cultures supplemented with cytokines (Lavau et al., 1997). We constructed lentiviral vectors expressing C-terminal siRNA for *Epm2a* or control sequence. Infection with a virus containing C-terminal siRNA for *Epm2a* resulted in complete silencing of the *Epm2a* gene in fibroblast (Figure 6A). Bone marrow cells from B10.BR mice pretreated with 5-fluorouracil (5-FU) were transduced with the siRNA or control viruses and selected for blasticidin-resistant transduced cells in the first plating in methylcellulose. Cells were cultured in vitro for four serial replatings, and the number of colonies was counted under a microscope. As shown in Figure 6B, the number of colonies formed from 10^4 vector-transduced bone

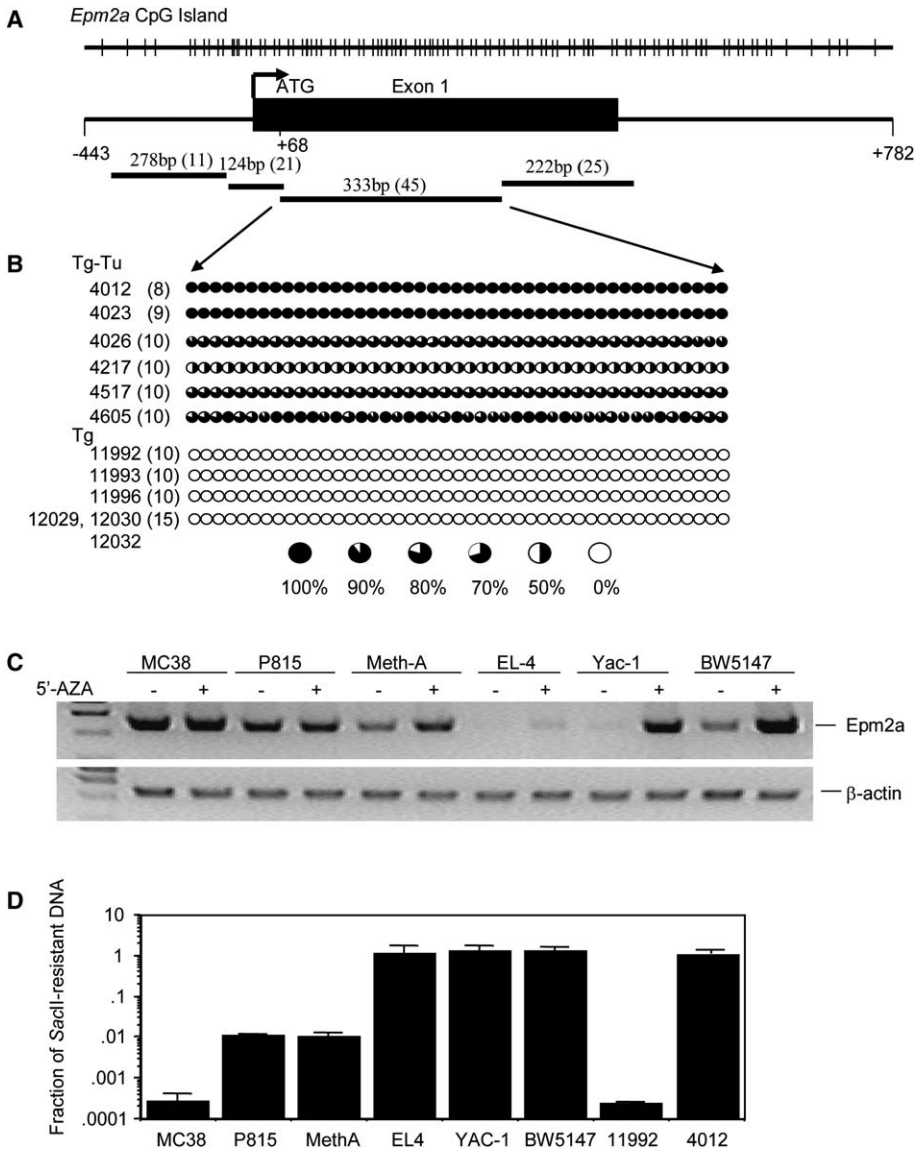

Figure 4. *Epm2a* is hypermethylated in lymphoma cells

A: Diagram of the 5′-CpG island and the four PCR fragments amplified using bisulfite-treated DNA to examine the methylation status of the *Epm2a* gene with number of CpG dinucleotides in each fragment indicated in parentheses.

B: Summary of the results of bisulfite sequencing of 333bp PCR products that contained 45 CpG dinucleotides. Fifty-seven clones were obtained from six lymphoma TG-B mice (Tg-Tu) (the mouse ID number is shown with clone numbers from each mouse labeled in parentheses), and 45 clones were obtained from six transgenic littermates without lymphoma (Tg). Each circle represents the methylation status of a CpG dinucleotide. Methylated and unmethylated alleles are shown as solid and open circles, respectively.

C: 5-Aza-dC-induced *Epm2a* expression in lymphoma cell lines (EL4, YAC-1, and BW5147), but not in three nonlymphoid tumor cell lines (colon cancer MC38, mastocytoma P815, fibrosarcoma Meth A).

D: *Epm2a* promoter methylation in lymphoma cell lines. The y axis is the fraction of the real-time PCR products from methylation-sensitive SacII-digested genomic DNA compared with that from undigested genomic DNA and is plotted in log scale. We used samples with 100% methylation (mouse 4012) and no methylation (mouse 11992) as determined in Figure 4B as positive and negative controls for the assay. The fraction between SacII post- and predigested samples with 100% methylation was defined as 1.0. All other samples were normalized accordingly. Data shown are means and SD of triplicate samples and have been repeated twice.

marrow cells was steadily reduced over serial replatings. In striking contrast, cells transduced with *Epm2a* siRNA had a drastic increase in the number of colonies in the third and fourth rounds, most of them tightly packed. These results demonstrate that silencing *Epm2a* drastically increases the self-renewal ability of the bone marrow stem cells.

To test whether silencing *Epm2a* in the bone marrow cells can cause hematological abnormality in vivo, we injected the siRNA-transduced or control vector-transduced BALB/c P1CTL TCR transgenic mouse (Sarma et al., 1999) bone marrow cells into irradiated syngeneic *RAG-2*$^{-/-}$ mice. The mice were examined 4 months after bone marrow reconstitution, as the mice in the siRNA group started to lose weight and had difficulty in breathing. The random integration of the viral constructs in the bone marrow cells was confirmed by Southern blot (Figure 6C). Examination of the bone marrow showed that in the chimera mice reconstituted with control vector-transduced bone marrow the myeloid over erythroid ratio was normal at 2. This ratio was drastically increased to 5.3 in four out of five recipients of siRNA-transduced bone marrow cells ($p = 0.004$) (Figure 6D). The increased M/E ratio was due to the increase in segmental and band neutrophils and decreased erythroid cells in the bone marrow. In addition, we observed an increased cellularity of the bone marrow in the siRNA-transduced group (Figures 6Ea and Eb). The fifth recipient of siRNA-transduced bone marrow had about 48% of monocytes and monoblasts in the bone marrow (Figure 6Ec) compared to less than 2% in the control group (Figure 6Ea), which is consistent with the diagnosis of chronic myelomonocytic leukemia. The cause of respiratory distress in the recipient mice that received siRNA-transduced bone marrow was due to a heavy infiltration of monocytic cells and fibroblastic proliferation in the lung tissue (Figure 6Ed). The homogenous infiltrating cells had abundant cytoplasm, large indented and lobulated nuclei that had one to three conspicuous nucleoli per nucleus, and active mitotic figures (Figure 6Ee). In order to confirm that the malignant infiltrating cells had integration of the lentiviral construct, we carried out a PCR in situ hybridization assay using the blasticidin resistance gene as probe. The results showed that the large cluster of infiltrating cancer cells contained the silencing vector (Figure 6Ef). These results,

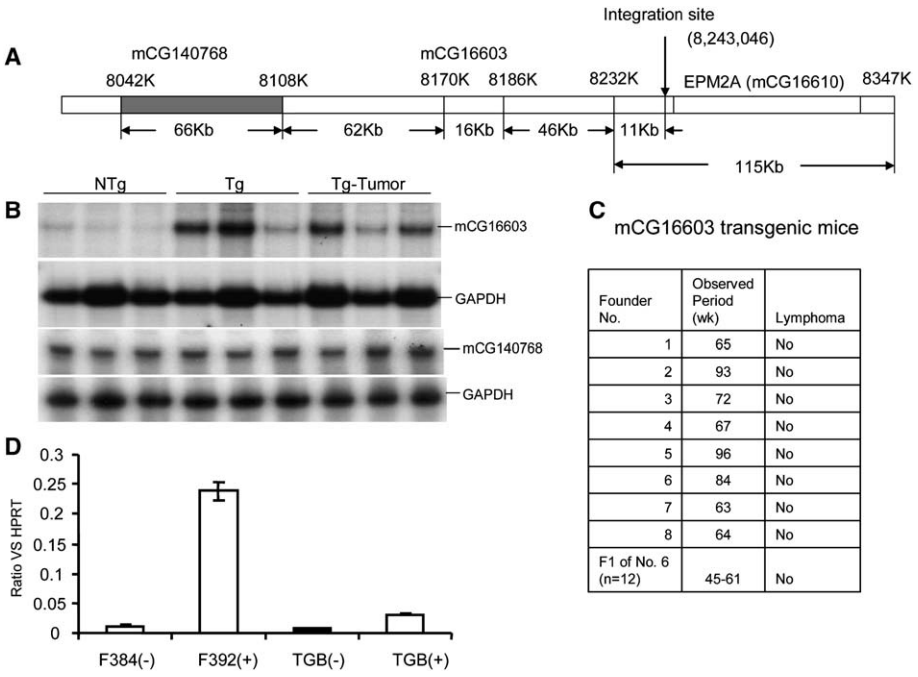

Founder No.	Observed Period (wk)	Lymphoma
1	65	No
2	93	No
3	72	No
4	67	No
5	96	No
6	84	No
7	63	No
8	64	No
F1 of No. 6 (n=12)	45-61	No

Figure 5. Overexpression of genes adjacent to the TCR transgene integration site does not lead to tumorigenesis

A: Genomic organization of *Epm2a* and the only two other genes within 300 kb of the integration site on chromosome 10. The cDNA designations are based on Celera database.

B: Expression of the two adjacent genes in nontransgenic littermates (Ntg), transgenic mice without tumor (Tg), and transgenic mice that developed tumor (Tg-Tu), as determined by RNase protection assay.

C: Summary of observation period of eight transgenic founder mice and 12 offspring of the founder 6 all express mCG16603 under the control of the proximal *lck* promoter.

D: The offspring of founder 6 (mouse F392) overexpress the mCG16603 gene, as determined by real-time PCR. Data shown are means and SD of triplicate samples and have been repeated twice.

taken together, demonstrate that silencing *Epm2a* resulted in myelodysplastic syndrome.

Since the above experiments involved mice or bone marrow that would produce only limited TCR repertoire, we have extended this analysis to determine whether immune deficiency is a precondition associated with cancer development. We first tested whether silencing *Epm2a* in the nontransgenic BALB/c bone marrow resulted in hematological abnormalities after the cells were used to reconstitute the RAG-2-deficient host. The BALB/c bone marrow successfully reconstituted the RAG-2-deficient mice, as demonstrated by the emergence of T cells, which could only be produced from donor cells. Pathological evaluation of the five recipients of *Epm2a*-silenced bone marrow at 4.5 months after transplantation revealed none of the abnormalities observed with the transgenic bone marrow. Thus, inactivation of *Epm2a* in bone marrow stem cells capable of yielding a full repertoire of T cells was insufficient to cause hematological abnormalities.

We also used vector control-treated or *Epm2a*-silenced B10.BR bone marrow to reconstitute the irradiated syngeneic B10.BR hosts in order to determine whether silencing *Epm2a* was sufficient to cause hematological malignancy. The B10.BR background was chosen, as it is the same as the TG-B mice except for the lack of the TCR transgene. In experiments involving a total of ten recipients in each group, we observed no hematological abnormalities over a 2.5–3.5 month period. Thus, even in the B10.BR background, silencing *Epm2a* was insufficient to cause hematological abnormalities unless the T cell repertoire was limited by the TCR transgene. Taken together, our results demonstrate that limited TCR repertoire rather than B10.BR background was required for tumor development associated with defects in *Epm2a*, although mice with pure B10.BR background were more susceptible.

To test whether the hematological malignancy in the TG-B mice could be complemented by *Epm2a*, we generated *Epm2a* transgenic mice (FVB background) under the control of the *lck* promoter. Although the FVB background was less susceptible to lymphoma than the B10.BR background, about 40% of the nontransgenic FVBxTG-B mice succumbed to lymphoma in 1 year. Complementation with the *Epm2a* transgene drastically decreased the incidence and delayed the onset of lymphoma (Figure 6F). Thus, *Epm2a* inactivation is both necessary and sufficient to initiate cancer development in vivo.

To test whether laforin can suppress the growth of other tumor cells, we transduced T lymphoma cell line BW5147 with either vector alone or *Epm2a*-containing lentiviral vectors. After a short-term drug selection, we compared vector and *Epm2a*-transfected tumor cells for their growth in vivo. As shown in Figure 6G, the overexpression of laforin in *Epm2a* transfectants had substantially reduced tumor growth in vivo. The tumor suppression depended on laforin's phosphatase activity, as inactivating mutation of the phosphatase (C265S) (Wang et al., 2002) abolished the tumor suppression. We also transfected the *Epm2a* cDNA into B104-1-1, a fibroblast cell line transformed by the P185neu oncogene (Schechter et al., 1984). We inoculated the *Epm2a* or vector transfected B104-1-1 cell lines into *RAG-2*$^{-/-}$ mice that lacked T and B lymphocytes. Based on the kinetics of tumor growth, it was clear that overexpression of *Epm2a* had a significant suppressive effect on B104-1-1 tumor growth (Figure 6H).

Laforin is the phosphatase for GSK-3β

Because laforin suppressed the growth of Her-2/Neu-transformed tumor cells, we explored the possibility that laforin may be involved in the PI-3K/Akt signaling pathway. We transfected *Epm2a* cDNA into NIH3T3 cells and evaluated the effect of laforin on platelet-derived growth factor (PDGF) receptor signaling. We first examined phosphorylation of Akt at Thr473 by 3′-phosphoinositide-dependent protein kinase (PDK) (Alessi et al., 1997). Activation and phosphorylation of PDK was not significantly affected by PDGF in the NIH3T3 cells, regardless of the expression of laforin. As a result of PDK recruitment, significant

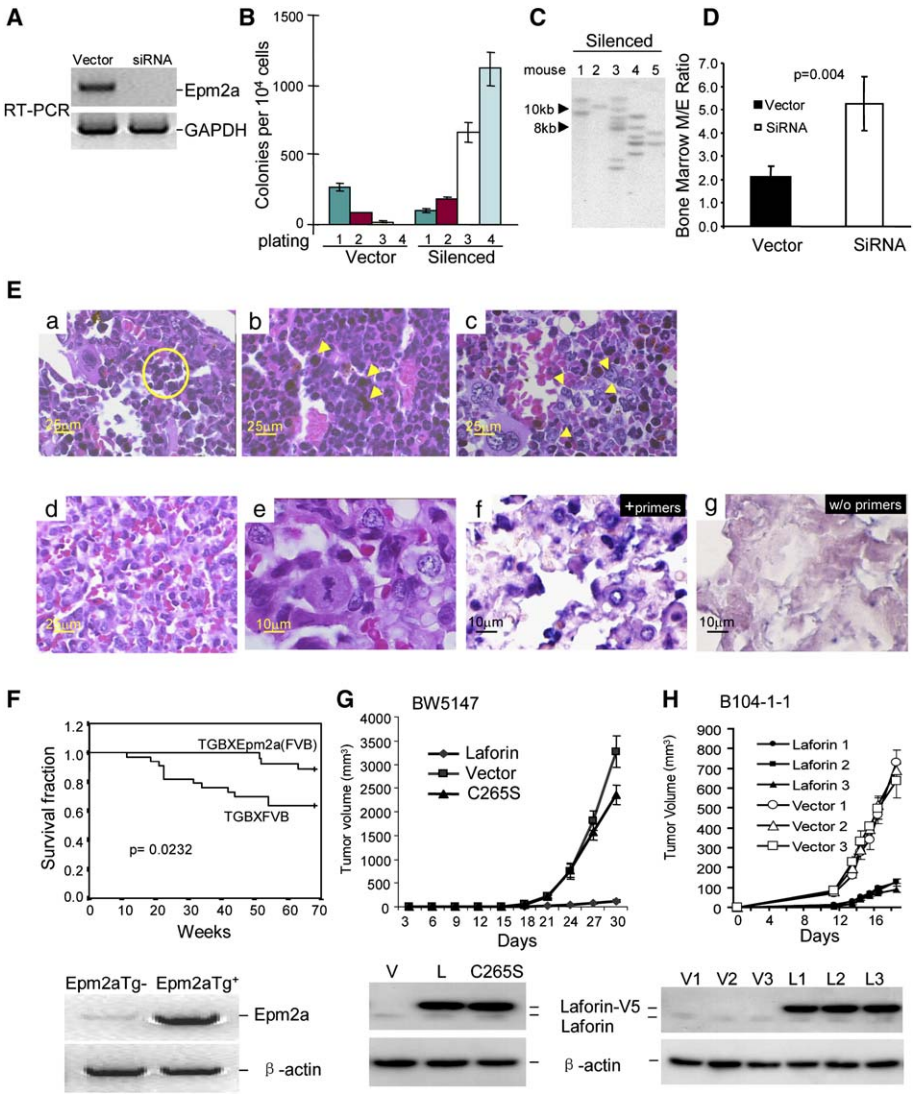

Figure 6. In vitro and in vivo transformation of bone marrow stem cells by silencing *Epm2a*

A: *Epm2a*-siRNA repressed Epm2a expression in NIH3T3 cells.

B: Silencing *Epm2a* in B10.BR bone marrow cells greatly increased self-renewal of bone marrow hematopoietic stem cells. The transduced bone marrow cells (10^4/well) were serially replated four rounds in methylcellulose, and blasticidin was added in first round. Data shown are means and SD of colony numbers in triplicate plates and are representative of three independent experiments.

C–E: Hematological disorders associated with silencing *Epm2a*. The irradiated RAG-2-deficient recipients of lentivirus-transduced bone marrow cells were sacrificed at 4 months after reconstitution. **C:** Southern blot using the blasticidin-resistant gene as probe showing random integration of the lentiviral vector in the *Epm2a*-silenced bone marrow. Note the distinct pattern in individual mice. **D:** Bone marrow cell counting showing different myeloid/erythroid (M/E) ratio in the recipients of the vector-transduced (n = 6) or siRNA-transduced (n = 4) bone marrow cells. The fifth case with a different presentation was not included. Data shown are means and SD. **Ea:** Representative histology of six vector-transduced bone marrow with clustered normoblasts (marked inside the circle). **Eb:** Representative histology of 4/5 of siRNA-transduced bone marrow with dispersed normoblasts (marked in arrows), increased cellularity with selective increase in band, and segmental neutrophils (M/E ratio is 5.8). **Ec:** The histology of the fifth recipient of siRNA-transduced bone marrow showing greatly increased (46% versus 2% in control bone marrow) and clustered monocytes and monoblasts (yellow arrows). **Ed:** Massive pulmonary infiltration and consolidation in lung tissues that completely obliterated the pulmonary parenchyma from recipients of siRNA-transduced bone marrow. **Ee:** High-power view of lung section showing heavy infiltration of malignant monocytic cells. A mitotic figure is present. **Ef:** PCR in situ hybridization (PCR-ISH) using a DNA probe of vector origin blasticidin resistance gene showing intensely positive signals on malignant infiltrating cells. **Eg:** A consecutive section, which received identical treatments but without PCR primers, was used as negative control.

F: *Epm2a* complementation suppresses tumorigenesis associated with the TG-B mice. *Epm2a* cDNA was inserted into transgenic vector with a proximal *lck* promoter. Founder mice with ectopic expression of *Epm2a* were crossed with the TG-B mice. The survival of the *Epm2a*$^+$ TG-B (n = 26) and *Epm2a*$^-$ TG-B (n = 33) littermates was observed over a 70 week period. The expression of *Epm2a* in *Epm2a*$^+$ and *Epm2a*$^-$ thymocytes as determined by RT-PCR is shown underneath.

G: Laforin suppresses the growth of murine T cell lymphoma BW5147. BW5147 cells were infected with empty vector only or with lentiviral vector of either wild-type or C265S mutant *Epm2a* cDNAs. Polyclonal stable transfectants were injected subcutaneously into the *RAG-2*$^{-/-}$ BALB/c mice (3×10^5 cells/mouse). The growth kinetics is presented. Data shown are means and SD, and represent those from two independent experiments. Expression of the V5-tagged laforin and the minute amounts of endogenous laforin are shown underneath.

H: Laforin suppresses the growth of the P185neu-transformed NIH3T3 cell line B104-1-1. B104-1-1 cells were transfected with either vector or *Epm2a* cDNA. Three stable clones from each group (Vector or Laforin) were injected into the *RAG-2*$^{-/-}$ BALB/c mice (3×10^5 cells/mouse). The growth kinetics is presented. Data shown are means and SD and are representative of two independent experiments. The expression of V5-tagged laforin and the minute amounts of endogenous laforin are shown underneath.

Akt phosphorylation was observed following PDGF stimulation, and again, this was only marginally affected by laforin expression (Figure 7A and Figure S1 in the Supplemental Data available with this article online). Interestingly, of the three downstream targets of Akt (Datta et al., 1999) that we examined, namely FKHR, AFX, and GSK-3β, only GSK-3β phosphorylation on Ser9 was affected by overexpression of laforin (Figure 7A). The effect was highly selective, as the phosphorylation of Tyr216 of GSK-3β and Tyr279 of GSK-3α was not affected by laforin, despite laforin's intrinsic dual specificity (Figure 7B). To determine the effect of laforin expression on GSK-3β activity, we precipitated GSK-3β and performed the in vitro kinase assay to test its ability to phosphorylate recombinant protein Tau, a known GSK-3β substrate (Cho and Johnson, 2003). As shown in Figure 7C, PDGF-induced inhibition of GSK-3β kinase activity was blocked in laforin-transfected cells. This was consistent with the effect of laforin on Akt-mediated phosphorylation of GSK-3β at Ser9.

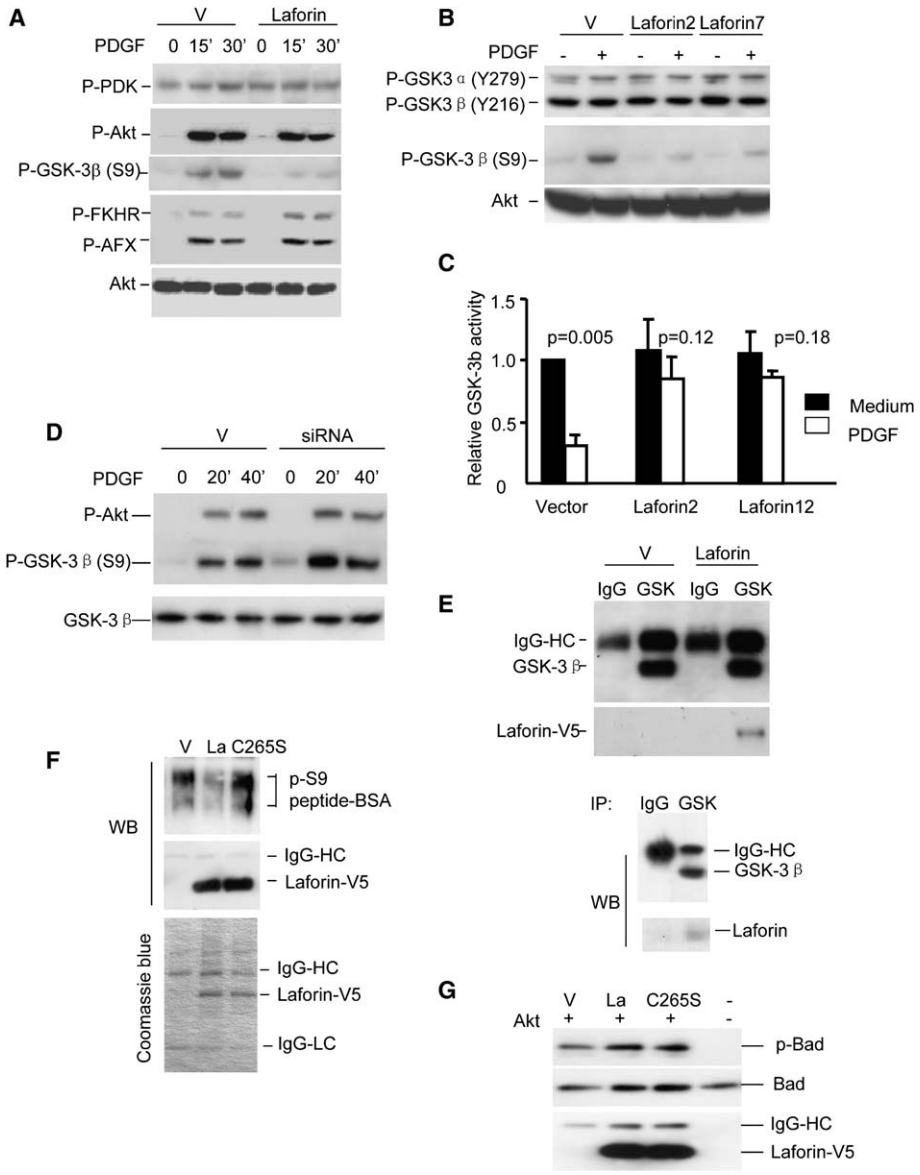

Figure 7. Laforin is a phosphatase of GSK-3β at Ser9

A: Laforin selectively prevented PDGF-induced phosphorylation of GSK-3β. Vector- or laforin-V5-transfected NIH3T3 cells were stimulated with PDGF for given periods of time. The activation of PDK (anti-P-Ser241), Akt (anti-P-Ser473), GSK-3β (anti-P-Ser9), FKHR (anti-P-Ser256), and AFX(anti-P-Ser193) was analyzed by Western blot. Total Akt was loading control.

B: Laforin dephosphorylated the P-Ser9 but not P-Tyr216 of GSK-3β and P-Tyr279 of GSK-3α. Two stable laforin-transfected clones are presented (laforin2 and laforin7).

C: Laforin prevented PDGF-induced inactivation of GSK-3β kinase activity. Vector- or laforin-transfected NIH3T3 cells were stimulated with PDGF for 30 min. The anti-GSK-3β immunoprecipitates were used for kinase assay to determine the GSK-3β kinase activity. Specific phosphorylation of recombinant Tau was determined by ^{32}P autoradiograph. The radioactive intensity in each lane was normalized based on the amounts of GSK-3β in each sample as determined by Western blot. The activity of the GSK-3β isolated from untreated vector transfectants was arbitrarily assigned as 1.0. Data shown are means and SD. Statistical difference was calculated by Student's t tests. Two stable laforin-transfected clones are presented (laforin2 and laforin12). Data shown are summary of three independent experiments.

D: siRNA suppresses endogenous laforin and enhances the PDGF-induced phosphorylation of GSK-3β. The activation of Akt (anti-P-Ser473) and GSK-3β (anti-P-Ser9) from vector- or siRNA-transfected NIH3T3 cells was analyzed. β-actin was the loading control.

E: Physical association between GSK-3β and laforin. Upper panel shows association of transfected laforin with GSK-3β. Vector- or laforin-transfected NIH3T3 cells were immunoprecipitated with either control IgG1 or anti-GSK-3β and blotted with anti-GSK-3β or anti-V5 for V5-tagged laforin. The lower panel shows association between GSK-3β and laforin in untransfected NIH3T3 cells. Laforin was detected by anti-laforin antibody.

F and G: Laforin dephosphorylates P-Ser9 of GSK-3β (**F**) but not P-Ser112 of Bad in vitro (**G**). P-Ser-9 peptide of GSK-3β was conjugated in bovine serum albumin (BSA), and recombinant soluble Bad protein was phosphorylated by constitutively activated Akt in the presence of ATP. The vector (V)-, *Epm2a* (L)-, or *Epm2a* mutant (C265S)-transfected HEK293 cells were lysed and immunoprecipitated with anti-V5 and mixed with substrates. The specific dephosphorylation was detected with anti-p-GSK-3β (Ser9) or anti-p-Bad (Ser112). Protein loading was confirmed by anti-V5 for laforin and anti-Bad. The protein composition of the precipitates was analyzed by SDS-PAGE and detected by Coomassie blue staining (**F**, lower panel). Data shown represent three independent experiments.

The selective effect of laforin on phosphorylation of GSK-3β at Ser9 raised the intriguing possibility that laforin may be the phosphatase of GSK-3β. We took three approaches to substantiate this hypothesis. First, we eliminated the endogenous laforin in NIH3T3 cells. Infection with a virus containing C-terminal siRNA for *Epm2a* resulted in complete silencing of the *Epm2a* gene in NIH3T3 cells (Figure 6A). As shown in Figure 7D, elimination of laforin expression had no effect on cellular levels of p-Akt, but as a result of siRNA inhibition of laforin, the p-GSK-3β became detectable even in the absence of PDGF. Furthermore, upon PDGF stimulation, levels of phospho-GSK-3β in cells treated with siRNA were higher than those found in vector-transfected control cells. In addition, the specificity of the knockdown was confirmed, as the biological effect was restored by reintroduction of human laforin, which had two base pair mismatches in the sequence targeted by the siRNA (Figure S2). Thus, laforin controls GSK-3β phosphorylation at Ser9.

Secondly, we evaluated whether GSK-3β and laforin can physically associate with each other. We treated the vector and laforin-transfected NIH3T3 cells with PDGF and immunoprecipitated GSK-3β protein with either control IgG1 or a monoclonal anti-GSK-3β antibody. The precipitates were analyzed by Western blot with either anti-GSK-3β antibody or the anti-V5 antibodies that detect the V5-tagged laforin protein. As shown in the upper panel of Figure 7E, anti-GSK-3β, but not control IgG1, brought down both GSK-3β and V5-tagged laforin

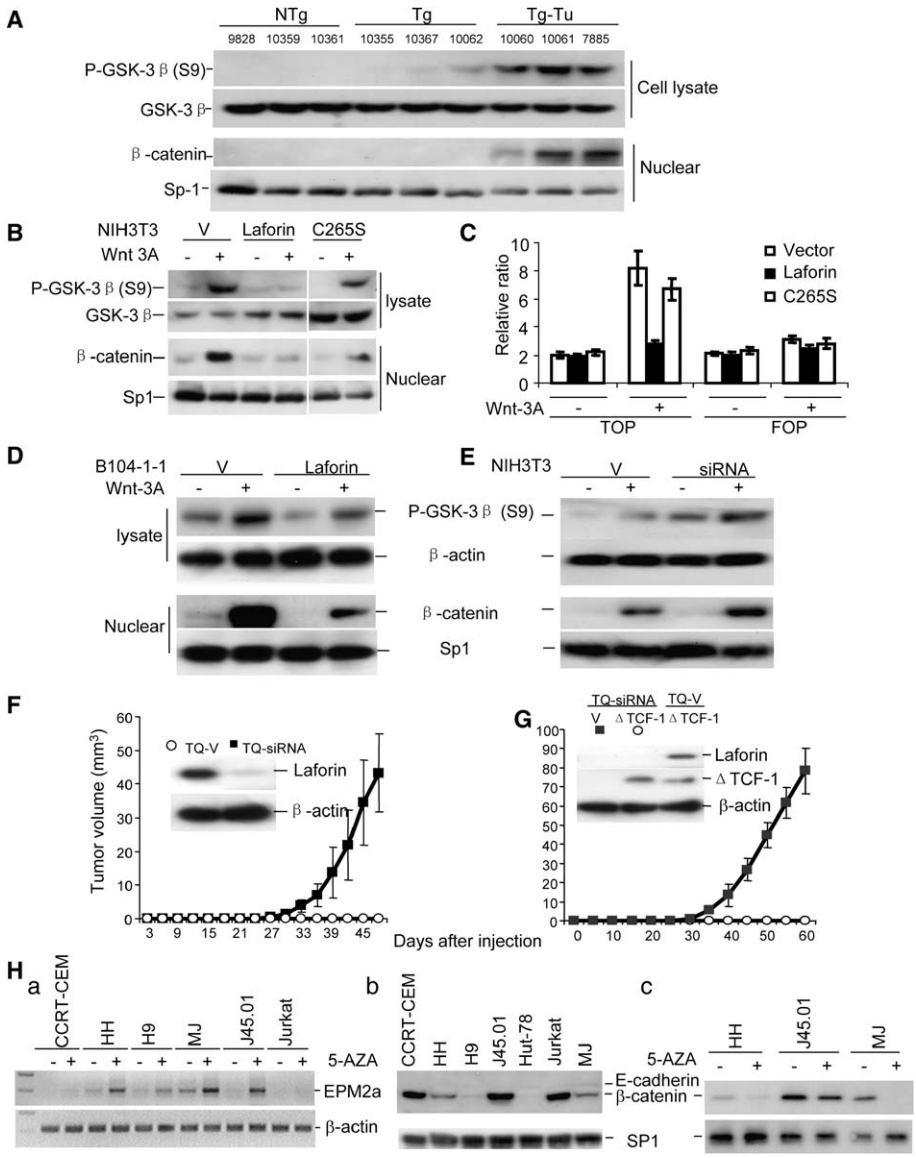

Figure 8. Laforin modulates the Wnt signaling pathway

A: Increased GSK-3β phosphorylation and β-catenin nuclear accumulation in the thymocytes from transgenic mice with lymphoma (Tg-Tu), but not the normal mice (NTg) and the transgenic mice yet to develop lymphoma (Tg).

B: Transfection of laforin suppressed Wnt signaling in NIH3T3 cells. NIH3T3 cells transfected with either vector or laforin were stimulated with Wnt-3A and tested for GSK-3β Ser9 phosphorylation and nuclear accumulation of β-catenin.

C: TCF reporter assay. pTOPFLASH or pFOPFLASH TCF luciferase reporter vector was cotransfected with pRL-SV40 Renilla control luciferase reporter plasmid into Vector (V), laforin, or mutant laforin (C265S) stably transfected NIH3T3 cells.

D: Laforin expression in tumor cell line B104-1-1 inhibited the GSK-3β Ser9 phosphorylation and β-catenin nuclear accumulation induced by recombinant Wnt-3A.

E: *Epm2a* siRNA increased the GSK-3β Ser9 phosphorylation and β-catenin nuclear accumulation induced by recombinant Wnt-3A in NIH3T3 cells.

F: siRNA silencing of laforin expression in the endothelial cell line LExF2-TQ increases its tumorigenicity. TQ cells infected with lentiviruses containing either vector or *Epm2a*-siRNA were injected subcutaneously into *RAG-2*$^{-/-}$ mice (1×10^6/mouse). The growth kinetics was recorded over a 2 month period. Data shown represent two independent experiments with three mice per group.

G: Increased tumorigenicity of the *Epm2a*-silenced LExF2-TQ cell line is eliminated by expression of a dominant-negative TCF-1 mutant (ΔTCF-1). As in **F**, except that the laforin-silenced TQ-siRNA cell line was supertransfected with either vector alone (V) or ΔTCF-1. The data shown are tumor growth kinetics with five mice per group. The levels of laforin and the ΔTCF-1 protein were determined by Western blot, and a control cell line expressing both ΔTCF-1 and laforin was used as control. Data shown are representatives of two experiments.

H: *EPM2a* expression and increased Wnt signaling in human T cell leukemia and lymphoma cell lines. **Ha:** *EPM2a* expression in human T lymphoma cell lines and the response to 5-Aza-dC treatment. RT-PCR was performed using primers that amplified the entire coding sequence of *EPM2a*, and β-actin was used as control. **Hb:** Increased nuclear accumulation of β-catenin in human T cell lymphoma cell lines. The nuclear extracts were isolated and blotted with anti-β-catenin and anti-E-cadherin. Nuclear protein Sp1 was used as loading control, and the absence of membrane marker E-cadherin indicates that the nuclear extracts were free of plasma membrane contamination. **Hc:** Induction of *EPM2a* correlated with reduced Wnt signaling. HH, J45.01, and MJ lines were treated with 5-Aza-dC for 36 hr, and the nuclear extracts were analyzed for β-catenin accumulation.

proteins in the *Epm2a*-transfected cells, but not in the vector-transfected cells. Thus, GSK-3β and laforin are associated in the NIH3T3 cells. To determine whether GSK-3β associates with endogenous laforin protein, we precipitated the GSK-3β in untransfected NIH3T3 cells and probed the precipitates with antibody specific for laforin. As shown in the lower panel of Figure 7E, significant amounts of laforin were coprecipitated with GSK-3β. Thus, laforin associates with GSK-3β under physiological conditions. The association between GSK-3β and laforin was independent of the phosphatase activity and was independent of stimulation by PDGF (Figure S3).

As a third approach, we tested whether recombinant laforin can directly dephosphorylate GSK-3β at Ser9 in vitro. We purified wild-type or mutant laforin protein with V5 tag from 293 transfectants by anti-V5 antibody coupled protein G beads. We used the BSA (bovine serum albumin)-coupled synthetic N-terminal peptide of the GSK-3β with phosphorylated Ser9 as substrate. Ser9-specific dephosphorylation was detected using antibodies specific for the phosphorylated GSK-3β Ser9. As shown in Figure 7F, the wild-type but not the C265S mutant laforin dephosphorylated the p-Ser9 peptide. The same laforin preparation, however, failed to dephosphorylate Bad, which was phosphorylated in vitro by a constitutively active recombinant Akt mutant protein (Figure 7G).

Laforin is an important modulator for Wnt signaling

GSK-3β is a major component in the Wnt signaling pathway (Cohen and Frame, 2001). To understand how laforin may suppress tumor growth, we tested whether it may modulate Wnt signaling by regulating GSK-3β activity. As shown in Figure 8A, in

transgenic mice that had one copy of the *Epm2a* inactivated, the thymocytes had a modest increase of phosphorylated GSK-3β in the cytosol, although no β-catenin was detected in the nuclei. In the lymphoma samples that had complete inactivation of the *Epm2a* gene, a drastic increase of GSK-3β phosphorylation and β-catenin accumulation in the nuclei were observed.

We carried out three lines of investigation to substantiate the notion that *Epm2a* may regulate Wnt signaling. First, we analyzed the effect of overexpressing or silencing the *Epm2a* expression in NIH3T3 cells. As shown in Figure 8B, Wnt induced GSK-3β Ser9 phosphorylation and accumulation of β-catenin in the nuclei of the vector-transfected cells. Both parameters were significantly inhibited by *Epm2a* overexpression. The phosphatase inactive *Epm2a* C256S abolished the function of laforin and restored the Wnt effect on GSK-3β Ser9 phosphorylation and nuclear accumulation of β-catenin. The functional importance of laforin expression in β-catenin activity was further confirmed by a TCR reporter assay (Korinek et al., 1997), as shown in Figure 8C. Likewise, expression of *Epm2a* in B104-1-1 cells inhibited GSK-3β Ser9 phosphorylation and nuclear accumulation of β-catenin, regardless of whether exogenous Wnt-3A was added (Figure 8D). We also observed a similar effect on T cell lymphoma BW5147, that transfection of *Epm2a*, but not phosphatase inactive *Epm2a*-C256S, suppressed nuclear accumulation of β-catenin (Figure S4). To test the role of endogenous laforin in Wnt signaling, we used siRNA to specifically silence the *Epm2a* gene in the NIH3T3 cell line. This resulted in a substantial increase of GSK-3β Ser9 phosphorylation and the nuclear β-catenin accumulation in NIH3T3 cells upon Wnt-3A induction (Figure 8E).

An interesting issue is whether the increased Wnt signaling was responsible for the tumorigenesis associated with *Epm2a* downregulation. We chose the TSC-2-deficient cell line LExF2-TQ (Inoki et al., 2003) to test this possibility, as it has increased β-catenin accumulation (Mak et al., 2003), but is not yet tumorigenic in immunodeficient mice (data not shown). More importantly, silencing *Epm2a* substantially increased Wnt signaling in this cell line (Figure S5). We first used the siRNA to silence *Epm2a* and injected the vector (TQ-V) and *Epm2a*-silenced (TQ-siRNA) cells into an immunodeficient host. As shown in Figure 8F, while the vector-transfected cells failed to produce tumors in the recipients, the *Epm2a*-silenced cells produced tumors in vivo. We then supertransfected the *Epm2a*-silenced cells with a dominant-negative TCF-1 (ΔTCF-1) to block the effector function of Wnt signaling. As shown in Figure 8G, ΔTCF suppressed tumor growth induced by silencing *Epm2a*. These results demonstrate that laforin suppresses tumor growth by inhibiting Wnt signaling.

As a first step in determining the relevance of our studies in human T cell lymphoma, we analyzed a panel of human T cell lymphoma cell lines for constitutive and 5-Aza-dC-inducible expression of *EPM2a* (Figure 8Ha) as well as accumulation of β-catenin in the nuclei (Figure 8Hb). Of the cell lines tested, CCRE-CEM, Jurkat, and J45.01 had no detectable *EPM2a* transcripts. Correspondingly, high levels of β-catenin were found in the nuclear extracts. In contrast, HH, H9, and MJ had detectable *EPM2a* transcripts and very low levels of nuclear β-catenin. Thus, the depression of *EPM2a* expression correlates strongly with enhanced Wnt signaling in human T lymphoma cell lines. To explore whether hypermethylation is responsible for the silencing of *EPM2a* in the T lymphoma, we treated these cell lines with nontoxic doses of 5-Aza-dC and evaluated expression of *EPM2a*. As shown in Figure 8Ha, in most of the cell lines tested, 5-Aza-dC caused a substantial increase in *EPM2a* expression. Moreover, induction of *EPM2a* expression correlates with reduced β-catenin (Figure 8Hc). Taken together, our data suggest that epigenetic repression of *EPM2a* may play a role in enhanced Wnt signaling in human T cell lymphoma.

Discussion

Laforin is a tumor suppressor in the mouse

We have presented several lines of evidence that support a role for laforin as a tumor suppressor. First, we have identified by position cloning that a line of TCR transgenic mice with rapid onset and high penetrance of lymphoma has the transgene inserted in the intron 1 of the *Epm2a* gene. Since the heterozygous mice had roughly 50% of laforin protein expression, it is likely that such insertion inactivated the *Epm2a* locus. The development of lymphoma was associated with complete silencing of *Epm2a*, which in turn was due to hypermethylation of the *Epm2a* promoter. Thus, the genetic lesion and epigenetic inactivation of the *Epm2a* gene during tumorigenesis was consistent with the new definition of a tumor suppressor gene (Paige, 2003). Second, we have demonstrated that hypermethylation of the *Epm2a* gene is not unique to the mouse lymphoma model in the TCR transgenic mice. Downregulation of laforin was observed in a large panel of mouse lymphoma cell lines and correlated with hypermethylation of the locus. Third, we have directly demonstrated that the transgenic complementation of *Epm2a* in the T cell lineage prevented the development of T cell lymphoma in the TG-B mice. Conversely, suppression of the *Epm2a* gene by siRNA increased tumorigenicity of an endothelial cell line, promoted self-renewal ability of bone marrow hematopoietic stem cells, and caused myelodysplasia in vivo. Taken together, our data demonstrate that *Epm2a* inactivation is both necessary and sufficient for the development of tumor in our mouse model.

It is of interest to note that while siRNA silencing primarily caused transformation of myeloid cells, essentially all lymphoma in the TG-B mice were derived from T cell lineage. Since the silencing of the other allele required methylation, and since the TCR transgene was turned on exclusively in the T cell lineage (even before cell surface TCR was detected), it is tempting to speculate that transcription of TCR locus may increase the likelihood of epigenetic silencing of the other *Epm2a* allele. On the other hand, siRNA silencing may disrupt *Epm2a* at the stem cell stage and may cause abnormal differentiation and transformation of myeloid cells, although the number of mice observed in the siRNA experiments was too small to exclude the possibility of other lineage of tumors.

An important feature of the *Epm2a* gene as a tumor suppressor is that it acts primarily in the immunocompromised host, as the *Epm2a*-associated tumor phenotype was observed in TCR transgenic mice that had extremely limited TCR repertoire. In support of this notion, we have been able to induce leukemia by silencing *Epm2a* only in bone marrow of TCR transgenic mice, but not when the bone marrow stem cells are capable of giving rise to a full repertoire of T cells. This notion would explain the lack of report on malignancy in mice with targeted mutation of *Epm2a* alone (Ganesh et al., 2002) and in the patients with

Lafora's diseases caused by homozygous mutations of the *EPM2a*. It is worth noting that LOH in 6q24, where the *EPM2a* resides (Minassian et al., 1998; Serratosa et al., 1995, 1999), is one of the most frequent chromosomal alterations in AIDS-related lymphoma (Pastore et al., 1996).

The immune system has long been suspected as a major barrier to tumorigenesis, as articulated by Ehrlich's hypothesis of immune surveillance (Dunn et al., 2004; Ehrlich, 1909). Despite newly emerged evidence for immune editing of cancers produced in immune competent hosts (Dunn et al., 2004), the issue remains controversial (Willimsky and Blankenstein, 2005), in part because of a lack of genetic lesions that can produce cancer only in an immunocompromised host. Our study demonstrates that inactivation of *Epm2a* is such a lesion.

Laforin is the phosphatase for GSK-3β and a critical modulator of Wnt signaling in tumor development

GSK-3β is a key modulator for several important signal transduction pathways. Although GSK-3β is inactivated by phosphorylation at the Ser9 position, it is unclear if the inactivated enzyme can be reactivated by dephosphorylation. While our study was being considered for publication, Lohi et al. showed that overexpression of *EPM2a* led to GSK-3β dephosphorylation at the Ser9 position (Lohi et al., 2005). However, it is unclear whether laforin is the specific GSK-3β phosphatase under physiological conditions. Here we provide strong evidence that laforin is a specific phosphatase for GSK-3β. First, laforin is constitutively associated with GSK-3β in vivo. Second, recombinant laforin protein isolated from either eukaryotic or prokaryotic cells specifically dephosphorylated Ser9 of GSK-3β, but not on unrelated Akt targets, such as Bad. Third, transfection of laforin reduced PDGF-induced phosphorylation of Ser9 of GSK-3β, but not that of Y216 of GSK-3β, Y279 of GSK-3α, or the phosphorylation of PDK, Akt, and other Akt substrates such as FKHR and AFX. Moreover, inactivation of *Epm2a* in either NIH3T3 cells or in TG-B mice substantially increased phosphorylation of GSK-3β. Finally, transfection of laforin substantially increased the enzymatic activity of GSK-3β. Taken together, our data demonstrate that laforin is a critical regulator of Ser9 phosphorylation and of the enzymatic activity of GSK-3β in vivo.

An important issue is whether, by regulating GSK-3β, laforin can modulate Wnt signaling. Since *Drosophila* appears to lack the *Epm2a* gene (Ganesh et al., 2001), it is unlikely that laforin is universally required for Wnt signaling. We have taken two approaches to demonstrate that laforin is an important regulator in Wnt signaling during tumor development. First, we showed that overexpression of laforin reduced nuclear accumulation of β-catenin in response to Wnt-3A, especially when PKC was activated. Conversely, knockdown of laforin both in tumor cell lines and in lymphomas that spontaneously arose in TCR transgenic mice resulted in a dose-dependent increase of β-catenin in the nuclei. Since nuclear accumulation of β-catenin plays a major role in tumorigenesis, modulation of Wnt signaling is likely to be responsible for the laforin-mediated suppression of tumor growth. Indeed, using a dominant-negative form of TCF-1, we showed that tumor growth associated with *Epm2a* silencing depends on Wnt signaling, which indicates that inactivation of *EPM2A* may be a critical event in cancer development in the context of immune suppression.

Experimental procedures

Antibody against laforin

Anti-laforin polyclonal antibody was produced by Genemed Synthesis, Inc. (San Francisco, CA). Rabbits were immunized with the synthetic peptide of 16 amino acid residues (YKFLQREPGGELHWEG, residues 85–100 in laforin protein, accession number AAD26336) coupled with keyhole limpet hemocyanin (KLH) in complete Freund's adjuvant. The antiserum was purified using peptide-conjugated Affigel column.

Mice

TG-B mice were housed and bred in OSU ULAR facility. BALB/c, B10.BR, and RAG-deficient mice were purchased from Jackson Lab. All animal experiments have been approved by OSU Institutional Animal Care and Use Committee (IACUC) and conformed to the national guidelines and regulations.

5-Aza-dC treatment

Cells were seeded at a density of 6×10^6 cells/10 cm plate and cultured with 5-Aza-dC (Sigma, St. Louis, MO) for 48 hr at maximal tolerable doses based on a 24 hr viability test (1 μM for P815, 2 μM for EL-4, 3 μM for BW5147, 10 μM for Yac-1 and Meth A, 20 μM for MC38; for human T leukemia and lymphoma cell lines: 8 μM for CCRT-CEM, 2 μM for H9, 4 μM for HH, 10 μM for Jurkat, MJ, J45.01, and Hut-78).

Epm2A siRNA constructs and lentiviral vectors

Oligonucleotides encoding siRNA directed against *EPM2a* at the C-terminal region of 934 to 954 nucleotides (5′-AAGGTGCAGTACTTCATCATG-3′) were subcloned into pSilencer 1.0-U6 siRNA expression vector (Ambion, Austin, TX) to generate *Epm2a*-siRNA according to the manufacturer's protocol.

Cell fractionation and β-catenin analysis

Vector, *Epm2a*, or siRNA transfectants of NIH3T3, B104-1-1, or LExF2-TQ cells were treated with or without recombinant mouse Wnt-3A protein (500 ng/ml, R&D Systems, Minneapolis, MN) in DMEM medium containing 1% serum (high-dose condition; Figures 8D and 8E) or Wnt3A (20 ng/ml) in conjunction with 0.5 μM PMA (Figure 8B and Figure S5) for 3 hr. The cells were either directly lysed for the detection of p-GSK-3β level in total lysate or homogenized and fractioned for the detection of β-catenin level in the nuclear extract in Western blots.

Methylcellulose bone marrow colony formation assay in vitro and bone marrow reconstitution in vivo

The in vitro methylcellulose bone marrow colony formation assay was performed according to a previously described protocol (Lavau et al., 1997). To test the in vivo transformation, the vector- or *Epm2a* siRNA-transduced bone marrow cells from BALB/c.P1CTL (Sarma et al., 1999) (a TCR transgenic strain without high incidence of lymphoma and syngeneic the *RAG-2*$^{-/-}$ recipient), BALB/c, or B10.BR mice were expanded in the medium containing the above cytokine cocktail for 2–7 days. The expanded bone marrow cells were i.v. injected into sublethally irradiated *RAG-2*$^{-/-}$ mice (2×10^6/mouse).

PCR in situ hybridization

The DNA probe was generated by amplifying the blasticidin-resistant gene from pLenti-V5-DTOPO vector (Invitrogen). Sections were prepared from formalin-fixed, paraffin-embedded tissue samples, and PCR in situ hybridization was carried out according to a previously described protocol (Nuovo et al., 1999). The PCR reaction was carried out with primers as follows: BLSD-F, AGC TTG TAT ATC CAT TTT CGG ATC TGA; BLSD-R, TAA AGG TAC CGA GCT CGA ATT GTG CTT. PCR reaction without primers was used as control.

Supplemental data

The Supplemental Data include Supplemental Experimental Procedures and five supplemental figures and can be found with this article online at http://www.cancercell.org/cgi/content/full/10/3/179/DC1/.

Acknowledgments

We thank Drs. Ming You, Kunliang Guan, Chunyu Wang, Joan E. Durbin, Bo Yuan, and Jin Fang for their helpful discussions and reagents; Dr. Shili Lin and Mr. Gary Phillips for statistical analysis; Lijie Yin for mice genotyping; and Lynde Shaw for secretarial assistance. This work is supported by a DOD grant (W81XWH-04-1-0704); an ACS grant (RSG-06-072-01-TBE); a grant from the Cancer Research Institute; and NIH grants CA82355 (to P.Z.), CA69091, CA58033, AI51342, and CA95426 (to Y.L.).

Received: December 14, 2005
Revised: May 10, 2006
Accepted: August 2, 2006
Published: September 11, 2006

References

Alessi, D.R., Deak, M., Casamayor, A., Caudwell, F.B., Morrice, N., Norman, D.G., Gaffney, P., Reese, C.B., MacDougall, C.N., Harbison, D., et al. (1997). 3-Phosphoinositide-dependent protein kinase-1 (PDK1): Structural and functional homology with the *Drosophila* DSTPK61 kinase. Curr. Biol. *7*, 776–789.

Boshoff, C., and Weiss, R. (2002). AIDS-related malignancies. Nat. Rev. Cancer *2*, 373–382.

Cho, J.H., and Johnson, G.V. (2003). Glycogen synthase kinase 3β phosphorylates tau at both primed and unprimed sites. Differential impact on microtubule binding. J. Biol. Chem. *278*, 187–193.

Cohen, P., and Frame, S. (2001). The renaissance of GSK3. Nat. Rev. Mol. Cell Biol. *2*, 769–776.

Datta, S.R., Brunet, A., and Greenberg, M.E. (1999). Cellular survival: A play in three Akts. Genes Dev. *13*, 2905–2927.

Dunn, G.P., Bruce, A.T., Ikeda, H., Old, L.J., and Schreiber, R.D. (2002). Cancer immunoediting: From immunosurveillance to tumor escape. Nat. Immunol. *3*, 991–998.

Dunn, G.P., Old, L.J., and Schreiber, R.D. (2004). The immunobiology of cancer immunosurveillance and immunoediting. Immunity *21*, 137–148.

Ehrlich, P. (1909). Über den jetzigen Stand der Karzinomforschung. Ned. tijdschr. geneeskd. *5*, 273–290.

Ganesh, S., Amano, K., Delgado-Escueta, A.V., and Yamakawa, K. (1999). Isolation and characterization of mouse homologue for the human epilepsy gene, EPM2A. Biochem. Biophys. Res. Commun. *257*, 24–28.

Ganesh, S., Agarwala, K.L., Ueda, K., Akagi, T., Shoda, K., Usui, T., Hashikawa, T., Osada, H., Delgado-Escueta, A.V., and Yamakawa, K. (2000). Laforin, defective in the progressive myoclonus epilepsy of Lafora type, is a dual-specificity phosphatase associated with polyribosomes. Hum. Mol. Genet. *9*, 2251–2261.

Ganesh, S., Agarwala, K.L., Amano, K., Suzuki, T., Delgado-Escueta, A.V., and Yamakawa, K. (2001). Regional and developmental expression of Epm2a gene and its evolutionary conservation. Biochem. Biophys. Res. Commun. *283*, 1046–1053.

Ganesh, S., Delgado-Escueta, A.V., Sakamoto, T., Avila, M.R., Machado-Salas, J., Hoshii, Y., Akagi, T., Gomi, H., Suzuki, T., Amano, K., et al. (2002). Targeted disruption of the Epm2a gene causes formation of Lafora inclusion bodies, neurodegeneration, ataxia, myoclonus epilepsy and impaired behavioral response in mice. Hum. Mol. Genet. *11*, 1251–1262.

Geiger, T., Gooding, L.R., and Flavell, R.A. (1992). T-cell responsiveness to an oncogenic peripheral protein and spontaneous autoimmunity in transgenic mice. Proc. Natl. Acad. Sci. USA *89*, 2985–2989.

Heng, H.H., Squire, J., and Tsui, L.C. (1992). High-resolution mapping of mammalian genes by in situ hybridization to free chromatin. Proc. Natl. Acad. Sci. USA *89*, 9509–9513.

Inoki, K., Zhu, T., and Guan, K.L. (2003). TSC2 mediates cellular energy response to control cell growth and survival. Cell *115*, 577–590.

Korinek, V., Barker, N., Morin, P.J., van Wichen, D., de Weger, R., Kinzler, K.W., Vogelstein, B., and Clevers, H. (1997). Constitutive transcriptional activation by a β-catenin-Tcf complex in APC−/− colon carcinoma. Science *275*, 1784–1787.

Lavau, C., Szilvassy, S.J., Slany, R., and Cleary, M.L. (1997). Immortalization and leukemic transformation of a myelomonocytic precursor by retrovirally transduced HRX-ENL. EMBO J. *16*, 4226–4237.

Liao, M.J., and Van Dyke, T. (1999). Critical role for Atm in suppressing V(D)J recombination-driven thymic lymphoma. Genes Dev. *13*, 1246–1250.

Liao, M.J., Zhang, X.X., Hill, R., Gao, J., Qumsiyeh, M.B., Nichols, W., and Van Dyke, T. (1998). No requirement for V(D)J recombination in p53-deficient thymic lymphoma. Mol. Cell. Biol. *18*, 3495–3501.

Lohi, H., Ianzano, L., Zhao, X.C., Chan, E.M., Turnbull, J., Scherer, S.W., Ackerley, C.A., and Minassian, B.A. (2005). Novel glycogen synthase kinase 3 and ubiquitination pathways in progressive myoclonus epilepsy. Hum. Mol. Genet. *14*, 2727–2736.

Mak, B.C., Takemaru, K., Kenerson, H.L., Moon, R.T., and Yeung, R.S. (2003). The tuberin-hamartin complex negatively regulates β-catenin signaling activity. J. Biol. Chem. *278*, 5947–5951.

Minassian, B.A., Lee, J.R., Herbrick, J.A., Huizenga, J., Soder, S., Mungall, A.J., Dunham, I., Gardner, R., Fong, C.Y., Carpenter, S., et al. (1998). Mutations in a gene encoding a novel protein tyrosine phosphatase cause progressive myoclonus epilepsy. Nat. Genet. *20*, 171–174.

Nuovo, G.J., Plaia, T.W., Belinsky, S.A., Baylin, S.B., and Herman, J.G. (1999). In situ detection of the hypermethylation-induced inactivation of the p16 gene as an early event in oncogenesis. Proc. Natl. Acad. Sci. USA *96*, 12754–12759.

Paige, A.J. (2003). Redefining tumour suppressor genes: Exceptions to the two-hit hypothesis. Cell. Mol. Life Sci. *60*, 2147–2163.

Pastore, C., Carbone, A., Gloghini, A., Volpe, G., Saglio, G., and Gaidano, G. (1996). Association of 6q deletions with AIDS-related diffuse large cell lymphoma. Leukemia *10*, 1051–1053.

Penn, I. (1995). Sarcomas in organ allograft recipients. Transplantation *60*, 1485–1491.

Penn, I. (1996). Malignant melanoma in organ allograft recipients. Transplantation *61*, 274–278.

Reimann, J., Rudolphi, A., Tcherepnev, G., Skov, S., and Claesson, M.H. (1994). TCR/CD3 ligation of a TCR-transgenic T lymphoma blocks its proliferation in vitro but does not affect its growth in vivo. Exp. Clin. Immunogenet. *11*, 197–208.

Rygaard, J., and Povlsen, C.O. (1974). Is immunological surveillance not a cell-mediated immune function? Transplantation *17*, 135–136.

Sarma, S., Guo, Y., Guilloux, Y., Lee, C., Bai, X.F., and Liu, Y. (1999). Cytotoxic T lymphocytes to an unmutated tumor rejection antigen P1A: Normal development but restrained effector function in vivo. J. Exp. Med. *189*, 811–820.

Schechter, A.L., Stern, D.F., Vaidyanathan, L., Decker, S.J., Drebin, J.A., Greene, M.I., and Weinberg, R.A. (1984). The neu oncogene: An erb-B-related gene encoding a 185,000-Mr tumour antigen. Nature *312*, 513–516.

Serratosa, J.M., Delgado-Escueta, A.V., Posada, I., Shih, S., Drury, I., Berciano, J., Zabala, J.A., Antunez, M.C., and Sparkes, R.S. (1995). The gene for progressive myoclonus epilepsy of the Lafora type maps to chromosome 6q. Hum. Mol. Genet. *4*, 1657–1663.

Serratosa, J.M., Gomez-Garre, P., Gallardo, M.E., Anta, B., de Bernabe, D.B., Lindhout, D., Augustijn, P.B., Tassinari, C.A., Malafosse, R.M., Topcu, M., et al. (1999). A novel protein tyrosine phosphatase gene is mutated in progressive myoclonus epilepsy of the Lafora type (EPM2). Hum. Mol. Genet. *8*, 345–352.

Shuman, S. (1994). Novel approach to molecular cloning and polynucleotide synthesis using vaccinia DNA topoisomerase. J. Biol. Chem. *269*, 32678–32684.

Wang, J., Stuckey, J.A., Wishart, M.J., and Dixon, J.E. (2002). A unique carbohydrate binding domain targets the lafora disease phosphatase to glycogen. J. Biol. Chem. *277*, 2377–2380.

Willimsky, G., and Blankenstein, T. (2005). Sporadic immunogenic tumours avoid destruction by inducing T-cell tolerance. Nature *437*, 141–146.